Binding of proton and iron to lignite humic acid size-fractions in aqueous matrix

doi: 10.1016/j.molliq.2018.01.104

The research article is originally published at *Journal of Molecular Liquids*
An Elsevier Journal
https://www.journals.elsevier.com/journal-of-molecular-liquids
The original publication is available at: https://doi.org/10.1016/j.molliq.2018.01.104

Binding of Proton and Iron to Lignite Humic Acid Size-Fractions in Aqueous Matrix

Zinnat A. Begum,[1, 2, *] Ismail M. M. Rahman,[1, *] Yousuke Tate,[3] Toshiharu Ichijo,[3] Hiroshi Hasegawa[4, *]

[1] *Institute of Environmental Radioactivity, Fukushima University, 1 Kanayagawa, Fukushima City, Fukushima 960-1296, Japan*

[2] *Department of Civil Engineering, Southern University, 739/A Mehedibag Road, Chittagong 4000, Bangladesh*

[3] *Denka Co., Ltd., Nihonbashi-Muromachi 2-chome, Chuo-ku, Tokyo 103-8338, Japan*

[4] *Institute of Science and Engineering, Kanazawa University, Kakuma, Kanazawa 920-1192, Japan*

*Author(s) for correspondence.

E-mail: zinnat.ara@gmail.com or r801@ipc.fukushima-u.ac.jp (ZAB);

immrahman@ipc.fukushima-u.ac.jp or i.m.m.rahman@gmail.com (IMMR);

hhiroshi@se.kanazawa-u.ac.jp (HH)

Abstract

The bioavailability of trivalent iron (Fe^{3+}) to plants can be enhanced using fertilizer solutions containing humic acids (HA) as manifested from the increased crop yield at an iron stress conditions. The lignite-derived HA ($HA_{lignite)}$ facilitates higher diffusion of Fe^{3+} between the soil layers as attributable to more number of reactive sites in the assemblage compared to those from other origins. In the current work, the proton-binding of $HA_{lignite}$ size-fractions (5–10, 10–30, 30–100, and >100 kDa), as segmented based on the molecular weight distribution, and their complexation with Fe^{3+} have been studied at varying pH ranging from low to high. The protonation or formation of Fe^{3+}-complexes exhibited a comparable pattern despite the differences in the conformational distribution of $HA_{lignite}$ size-fractions. The protonation behavior specified that the behavior of $HA_{lignite}$ size-fractions has similarity with that of a dibasic acid. The results are interpreted using reactive structural units (RSU) concept to show that the carboxyl and phenolic-hydroxyl groups in the $HA_{lignite}$ size-fractions simultaneously available as the Fe^{3+}-binding sites. The stability constants for larger MW fractions of $HA_{lignite}$ (>100 kDa) was the lowest, as attributed to the increased aggregation rate in an aqueous matrix. The trend in conditional stability constants of $HA_{lignite}$-size fractions and other Fe-chelators point to a better Fe-binding capability of $HA_{lignite}$ (30–100 kDa) size-fraction than the biodegradable alternatives (GLDA, HIDS, EDDS, IDSA, or NTA), while the Fe-interaction was stronger with classical synthetic chelators (EDTA, DTPA, or EDDHA).

Keywords: Iron; Lignite-derived humic acids; Protonation; Complexation; Bioavailability

1.0 Introduction

Iron (Fe) was recognized as an essential nutrient for plants because of its significant role in the photosynthesis, nitrogen fixation, hormone production, or several other cellular activities in plants [1, 2]. The widespread abundance of Fe in soils, fourth-most to be precise, however, cannot ensure the supply of adequate Fe to plants due to the formation of sparingly soluble Fe^{3+} species, such as $Fe_2O_3{\cdot}nH_2O$, $Fe(OH)_2^+$, $Fe(OH)_3$, and $Fe(OH)_4^-$ in aerobic environments [3, 4]. The Fe-stress conditions has been accomplished in plants by any of the following routes: a) Fe-solubilization using proton-release, reducing agent secretion and membrane-bound Fe^{+3} reductase oxidase activity followed by diffusion of Fe to roots with an iron-regulated-transporter, (b) Fe-binding to root-released phytosiderophore to form soluble complexes as recognizable to specific membrane transporters [5-7]. The lack in Fe-nutrition impedes crop growth or yields despite the plant physiology factors, and the alleviation approaches include bioavailability escalation of indigenous soil-Fe, supplement with an external iron-available solution or modification of Fe-uptake mechanisms in plants [4].

The characteristics of synthetic chelators in keeping metal ions at solutions within a wider pH range were exploited to facilitate the increased-diffusion of already available Fe in soils or to supply as Fe-chelates with the fertilizer solutions [8, 9]. The application of EDTA, DTPA, EDDHA in liquid formulations to increase the bioavailability of soil-Fe to plants has been introduced since the 1950s [10]. The prolonged persistence of the classical Fe-chelators with a harmful impact on the surrounding biota evoke concerns [11, 12], which were proposed to be abated using eco-friendly alternatives (e.g., GLDA, HIDS, EDDS, or IDSA) [13-17]. The rapid biodegradation of the Fe-chelators [18, 19], nevertheless, can be a limiting factor considering the time-lag required for fertilizer to complete its role as a metal complexone [4, 13].

The organomineral fertilizers primarily consist of humic substances (HS) [20, 21], as isolated from naturally oxidized lignite derivatives [22], enhance the rates of seed germination, nutrient uptake, root growth, and crop yields [23-25]. The effect of HS in

increasing bioavailability of plant-micronutrients (e.g., Fe, Zn, Mn, and so forth) was attributable to the complexation between HS and metals [26]. The HS also aids in the diffusion of plant-nutrients among the soil-layers and uptake in plants without any negative impact [21, 26, 27]. A higher bioavailability of HS-Fe complexes than those with EDTA [28], desferrioxamine B or ferrichrome [29] has also been reported. An increase in Fe-bioavailability to plants with the lignite-derived HS application compared to those from other origins has also been observed [30]. The humic (HA) and fulvic acids are the acid-base reactive fractions in the HS that are usually separated using their corresponding solubility in alkalis and acids [22].

The proton- and metal-binding behavior of HS in solution have been an issue of interest because of their role in the acid-base equilibria of natural aqueous systems, and impact of solution pH on the complexation between metal and HS [31]. The acid-base equilibria of –COOH (carboxyl), Ph-OH (phenolic-hydroxyl) groups control the proton- or ion-binding properties of HS, which can be measured using potentiometric titrations as reported earlier for natural-source-derived HS [27, 31, 32].

The structural chemistry of lignite-derived HA ($HA_{lignite}$) is different from those derived-from other origins because of the extensive-pretreatments with oxidizing reagents or mineral acids of the parent materials [20], which increases the contents of oxygenated functional groups, such as carboxyl, phenolic-hydroxyl and carbonyl (>C=O), as well as the reactivity or solubility of the HA [22]. Thus, the $HA_{lignite}$ could offer several reactive sites for ion-binding [32], and interactions could occur through the water-bridge formation, electrostatic bonding with COO^- group, coordinate linkage with a single donor functional group, or combined-chelation in carboxyl and phenolic-hydroxyl sites [4]. The HAs are assumed to be an assorted-assemblage of several smaller molecular fragments that are bound by weak dispersive forces, such as, van dar waals, π–π or CH–π interactions and so forth, to form supramolecular aggregates [33]. The disparity in conformational distribution among the $HA_{lignite}$ size-fractions via molecular characterization [34], or the corresponding impact of $HA_{lignite}$-fractionation on iron solubility [35] has been reported.

The current work aimed to study the proton- and iron-binding behavior of $HA_{lignite}$ size-fractions in the aqueous matrix, which has not been reported before. The results supposed to extend the knowledge on the suitability of $HA_{lignite}$ size-fractions compared to the classical or biodegradable Fe-chelators as a micronutrient carrier in soil environment.

2.0 Experimental

2.1 Reagents

The $HA_{lignite}$, as supplied by Denka Co., Ltd. (Tokyo, Japan), was isolated from lignite samples of Berezovsky, Russia using an HNO_3-assisted degradation followed by a modified version of the IHSS recommended scheme [36]. The ultimate analysis of the dried (at 105°C) $HA_{lignite}$ sample using a CHN-O analyzer (Flash 2000; Thermo Scientific, Waltham, MA, USA) confirmed the following elemental composition (wt%): C, 52.0; H, 3.8; N, 4.0; O, 34.6. The distribution of carbon in the functional groups was determined using the protocols from Tsutsuki, *et al.* [37] to confirm the following (mmol g^{-1} C): OH + COOH, 13.9; COOH, 12.3.

The $HA_{lignite}$ was subsequently fractionated in a Vivaflow 200 system (Sartorius Stedim, Surrey, UK) using tangential-flow ultrafiltration technique. The Fig. S1 (Appendix A: Supplementary information) shows the complete scheme for $HA_{lignite}$ isolation and $HA_{lignite}$ fractionation. The average molecular weight and total organic carbon content in the $HA_{lignite}$ size-fractions are listed in Table 1.

All the other chemicals or solvents are of analytical reagent grade. Titrisol® iron standard ($FeCl_3$ in 15% HCl) (Merck KGaA, Darmstadt, Germany) was used to prepare the iron stock solution. The carbonate-free potassium hydroxide (KOH) (Kanto Chemical, Tokyo, Japan) was standardized using potassium hydrogen phthalate (Wako Pure Chemical, Osaka, Japan. The pre-standardized hydrochloric acid (HCl) (Kanto Chemical, Tokyo, Japan) solution was used for neutralization of the initially added KOH in $HA_{lignite}$ samples. The potassium chloride (KCl) (Wako Pure Chemical, Osaka, Japan) was used to adjust the solution ionic strength (*I*).

2.2 Sample preparation and potentiometric measurements

The $HA_{lignite}$ solutions in the aqueous matrix (50 cm^3, total volume) were prepared at the following compositions: (a) $HA_{lignite}$, 160 mg L^{-1} + HCl, 0.1 mol·dm^{-3} + KCl, 1.0 mol·dm^{-3}; (b) solution (a) + Fe^{3+}, 1.0×10^{-3} mol·dm^{-3}. The solution (a) was used to determine the protonation constants, and the solution (b) was used for the determination of stability constants $HA_{lignite}$-Fe systems. The intermolecular interactions between the ionic charges occur more effectively in the solvent systems at $I \geq 0.1$ mol·dm^{-3} due to the compressed ionic atmosphere [38, 39], which prompted to select I = 0.1 mol·dm^{-3} for all the experiments.

The solution systems have been titrated with 0.1 mol·dm^{-3} carbonate-free KOH using the KEM AT-710 automatic titrator (Kyoto Electronics; Kyoto, Japan). The potentiometric titration assembly includes a pH-combination electrode, a temperature probe, and a magnetic stirrer. The solutions were placed in a sealed vessel (100 cm^3) containing electrode, temperature probe, and titrant dosing nozzle inlets, plus in-out options for N_2 gas. The solution in vessel was placed in the SKG-01 jacketed heat exchanger bath (AS ONE, Tokyo, Japan), while the system temperature was maintained at 25 ± 0.1°C using a combination of the TBK202HA constant temperature water heater (Advantec, Tokyo, Japan) and the Eyela CTP-1000 thermo-controlled water circulator (Tokyo Rikakikai, Tokyo, Japan). The flow of N_2 gas was continued through the solution system to eliminate the CO_2 ingress and to achieve inert atmosphere. The standard pH solutions (Horiba Scientific, Kyoto, Japan) were used to calibrate the electrode at pH 4.0, 7.0 and 9.0 before each titration. The electrode can measure solution pH up to the third decimal place of pH units with a precision of ± 0.001, and the potential were simultaneously recorded with a precision of ± 0.1 mV. The rate of drift of the electrode was recorded over a pre-fixed interval (3 min) with a constant increment of titrant volume (0.02 mL), and an adequate mixing of the components was ensured through continuous stirring. The titrant addition was continued, starting from pH 2.5, until the solution pH changes to 11, as achieved within an average time-lag of 14 ± 2 h, to obtain a real-time titration curve from the

recorded data. All the titrations were carried out from the acid side due to the presumed possibility of higher pH limit of system homogeneity in such a case [40]. Each experiment was repeated at least five times, and the potentiometric data points used for analysis were not less than 150.

2.3 Calculation

The experimental potentiometric data-sets (See Table S1, Appendix A: Supplementary information) were processed with the following computation software: GLEE 3.0 [41], Hyperquad2008 [42] and HySS2009 [43].

The GLEE (Glass Electrode Evaluation) program was used to include the impact of electrode junction potentials on the potentiometric measurements in high acidic or basic regions. The data were refined through the non-linear least-square approach to fit a modified *Nernst* equation, as shown below:

$$E = E^0 + s \log_{10}[\mathrm{H}^+] \quad (1)$$

In Eq. (1), E, E^0, s and $[\mathrm{H}^+]$ represents, respectively, measured electrode potential, standard electrode potential, slope and hydrogen ion concentration, while E^0 and s are parameters of the refinement. This program also estimates the extent of carbonate contamination, if any, in the base solution.

The Hyperquad2008 program was used to determine the protonation and complexation constant from the potentiometric data by minimizing fitting criteria between observed and expected titration data based on the non-linear least-square approach as defined using the following relation:

$$\chi^2 = \sum \frac{(\text{Calculated data} - \text{Observed data})^2}{\text{Observed data}} \quad (2)$$

The constant values were obtained as 'overall formation constant (β_{pqr}),' while p, q, and r represent, respectively, the stoichiometric coefficients for Fe^{3+} (M), H (proton), and L ($HA_{lignite}^{2-}$) in the solution at equilibrium. The overall stoichiometry associated with the possible equilibria in solution can be described using the following equation:

$$p\mathrm{M} + q\mathrm{H} + r\mathrm{L} \leftrightharpoons \mathrm{M}_p\mathrm{H}_q\mathrm{L}_r \qquad \beta_{pqr} = \frac{[\mathrm{M}_p\mathrm{H}_q\mathrm{L}_r]}{[\mathrm{M}]^p[\mathrm{H}]^q[\mathrm{L}]^r} \quad (3)$$

However, if a system has two or more equilibria, the stability constants can be defined by considering the stepwise addition of one $HA_{lignite}$-species at a time or for the addition of all at once.

$$[ML] = \beta_1[M][L] \quad (4)$$

$$[ML_2] = \beta_2[M][L]^2 \quad (5)$$

β_1 denote the stepwise formation constant in Eq (4), and β_2 represent the overall formation constant in Eq (5). The calculated values of protonation and complexation constants those have a good fit with the observed ones, and the corresponding standard deviation values were obtained after the data processing with Hyperquad2008.

Hydrolysis of a metal ion in the aqueous matrix is considered to be a competitive process [40] and, therefore, the values of complexation constants for Fe-$HA_{lignite}$ systems were further corrected for the hydrolysis of Fe ions in solution. The hydrolysis constant of iron species [44] was added as invariable parameters to the Hyperquad2008 program to facilitate the programmed-correction of complexation constants that are calculated as variables.

The HySS (Hyperquad Simulation and Speciation) program was primarily used to simulate the titration curves at varying experimental conditions, as well as to provide the speciation diagrams.

3.0 Results and discussion

3.1 Protonation behavior of the $HA_{lignite}$ size-fractions in solution

The $HA_{lignite}$ size-fractions contained an appreciable proportion of carboxyl, phenolic-hydroxyl and carbonyl groups (see FT-IR spectra in Fig. S2, Appendix A: Supplementary information). The titration curves (Fig. 1) and speciation diagrams (Fig. 2) for the $HA_{lignite}$ size-fractions were similar to the behavior of dibasic acids with distinctly separated buffer areas. The proton-dissociation from carboxyl groups assumed to occur in the acid-region, while the dissociation of phenolic-hydroxyls corresponded to that of in the high-pH regions. Therefore, the proton-dissociation equilibria of $HA_{lignite}$ size-fractions in the lower and

higher pH-regions, imitating the behavior of all carboxyl and phenolic-hydroxyl groups respectively, can be predicted considering the interaction with two functional group-sites (Fig. 3).

The proton-binding constants of the $HA_{lignite}$ size-fractions determined from the acid-base titration data are listed in Table 2. The protonation behavior of the $HA_{lignite}$ size-fractions was not significantly different (pK_1, 2.7~3.0, pK_2, 10.4~10.7; T, 25 °C; I, 0.1 mol·dm^{-3}), indicating negligible impacts due to the molecular size differences or compositions. The concept of reactive structural units (RSUs) has been used to calculate the empirical proton-binding constants of $HA_{lignite}$, while all the RSUs contain at least one group with acid-base functionality [32]. The empirical proton-binding constants in the acidic-region as calculated for the salicylic acid (pK_1, 2.80; T, 25 °C; I, 0.1 mol·dm^{-3}) and acetoxyacetic acid (pK_1, 2.81; T, 25 °C; I, 0.1 mol·dm^{-3}), two of the representative RSUs in natural organic molecules [45, 46], has shown comparable protonation constants [47] to that observed in the current work (pK1 ($HA_{lignite}$, 5-10 kDa): 2.8, pK1 ($HA_{lignite}$, 10-30 kDa): 2.78, pK1 ($HA_{lignite}$, 30-100 kDa): 3.04, pK1 ($HA_{lignite}$, >100 kDa): 2.67; T, 25 ± 0.1 °C; I, 0.1 mol·dm^{-3}).

3.2 Stability constants of the $HA_{lignite}$ size-fractions with iron

The overall binding constants (logβ_{pqr}) for the ML systems (M, Fe^{3+}; L, $HA_{lignite}^{2-}$) were computed from the potentiometric titration data (Table 3). The solution pH controls the distributions of ML species in the aqueous matrix at varying equilibrium conditions to regulate the corresponding bioavailability or physiological activities [48]. The distribution of ML species in the pH range of 2.0 to 12 (T, 25 ± 0.1 °C; I, 0.1 mol·dm^{-3}) for all the $HA_{lignite}$ size-fractions (Fig. 4) confirmed that the complexation was started from the high-acidic region. The formation of ML^+ was observed from pH < 2 to ~6. The Fe^{3+} usually exist as $[Fe(H_2O)_6]^{3+}$ species at strongly acidic conditions in the $HA_{lignite}$ and Fe^{3+} solution mixtures. The water molecules in $[Fe(H_2O)_6]^{3+}$ retracted with the increasing solution pH via KOH addition initiating complexation at pH < 2 to form ML^+ species. As the pH increases, the more aqua ions are released to bind another $HA_{lignite}$ unit to form ML_2^- that

occurred from pH <2 to ~11 (M, Fe^{3+}; L, $HA_{lignite}^{2-}$), while the $M(OH)_4^-$ was appeared from pH 9. The dominant species within the ML systems (M, Fe^{3+}; L, $HA_{lignite}^{2-}$) was ML_2^- occurring at a rate of 50–98% almost in the entire pH range (3 to 10.5).

The metal-binding in natural humic substances was assumed to occur at the salicylic acid-like bidentate sites based on chemical studies suggesting that carboxyl and phenolic-hydroxyl groups simultaneously participate in metal chelation, while alcoholic-hydroxyl does not [49, 50]. A schematic representation is thus provided to explain the interaction of RSUs consisting of carboxyl and phenolic-hydroxyl groups offering bidentate chelating sites to Fe^{3+} ions (Fig. 5). There is a possibility of Fe-interaction at multiple reactive sites of $HA_{lignite}$ due to the heterogeneous distribution of functional groups, and the formation of ML_2 can be observed as well (Fig. 6).

The stepwise formation constants ($\log K_{FeL}$) was calculated from the differences between the $\log\beta$ values for each of $HA_{lignite}$ size-fraction (Table 4), and compared with other iron-chelators for agriculture [13]. The $\log K_{FeL}$ values observed for $HA_{lignite}$ size-fractions are comparable with that reported by Perrin [51] for salicylic acid (Table 4), which has been suggested as the general humic substance analog [46]. The gallic acid (GA) has also been used as an appropriate model to study the radical properties of humic acids [52], and the $\log K_{FeL}$ values for the Fe-GA systems [53-55] are somewhat comparable (Table 4) with those of Fe-$HA_{lignite}$.

The comparative $\log K_{Fe}$ for the ML species with different $HA_{lignite}$ size-fractions indicated the lowest value for larger MW fractions of $HA_{lignite}$ (>100 kDa). It could be correlated with the increased aggregation rate of corresponding $HA_{lignite}$ size-fraction in the aqueous matrix [35, 56], either attributable to intermolecular H-bond formation via the protonation of $HA_{lignite}$ functional groups [57] or to the charge neutralization and cation bridge formation [58].

3.3 Conditional stability constants of the $HA_{lignite}$ size-fractions with iron

The $\log_{10}\beta_{pqr}$ indicate fundamental stability characteristics of an ML species in solution [59]. However, the system equilibria frequently altered due to solution pH, interfering elements in

the matrix, and so forth, which were included to define the term 'conditional stability constant ($\log_{10}K'_{ML}$)'.

$$\log_{10}K'_{ML} \leftrightharpoons \log_{10}K_{ML} - \log_{10}\alpha_{HL} - \log_{10}\alpha_{M} + \log_{10}\alpha_{ML} \quad (6)$$

The complexation constants for ML species was expressed using $\log_{10}K_{ML}$ in Eq (6), while the effects due to the side reactions were denoted using $\log_{10}\alpha_{HL}$ (protonation of chelator), $\log_{10}\alpha_{M}$ (formation of metal hydroxides), and $\log_{10}\alpha_{ML}$ (formation of metal-proton-chelator or metal-hydroxo-chelator species) [60].

The $\log_{10}K'_{ML}$ values for Fe-complexes with $HA_{lignite}$-size fractions were calculated using HySS2009 [43] for pH range 2 to 12. The $\log_{10}K'_{ML}$ values for salicylic acid, GLDA, HIDS, EDDS, IDSA, NTA, EDTA, DTPA, and EDDHA were also computed using the corresponding $\log_{10}K_{ML}$ values, as extracted from literature [47, 51, 61, 62], and compared with that of the current work (*T*, 25 ± 0.1°C; *I*, 0.1 mol·dm^{-3}; matrix, H_2O) (Fig. 7). The average trend in the $\log_{10}K'_{ML}$ distribution was as follows: EDDHA > DTPA > EDTA > $HA_{lignite}$ (30–100 kDa) > EDDS > $HA_{lignite}$ (10–30 kDa) > $HA_{lignite}$ (5–10 kDa) > $HA_{lignite}$ (>100 kDa) > Salicylic acid > NTA > HIDS > GLDA > IDSA. A stronger interaction of Fe with the classical chelators (EDTA, DTPA, and EDDHA) was observed throughout, which application has been an issue of concern due to the eco-safety issues [63]. However, the $HA_{lignite}$ size-fractions has better Fe-binding capability than the general humic substance analog salicylic acid and other eco-friendly biodegradable iron-chelators (e.g., NTA, HIDS, GLDA, and IDSA), while EDDS has comparable performance. Moreover, a $\log_{10}K'_{ML}$ value of 6 or above, which is favorable for efficient complexation [64], has been observed in the pH range of 2 to 9 for all $HA_{lignite}$ size-fractions.

4.0 Conclusion

The interactions of $HA_{lignite}$ size-fractions (5–10, 10–30, 30–100, and >100 kDa) with trivalent Fe regarding the stability of corresponding Fe-$HA_{lignite}$ complexes have been studied. The $HA_{lignite}$ fractionation based on molecular weight distribution was assumed to have an impact on complexation or protonation behavior, while the experimental results

indicated the opposite. The stability of Fe-complexes showed an increasing pattern with the increase of $HA_{lignite}$ size-fractions, while the value was lowest with >100 kDa. The dibasic acid type protonation behavior confirmed the simultaneous chelation in carboxyl and phenolic-hydroxyl group positions of RSUs within the heterogeneous assemblage of $HA_{lignite}$. The proton-binding constants of $HA_{lignite}$ size-fractions at the lower pH region and the constants for Fe(III)-binding were comparable with the values observed for the general humic substance analog salicylic acid. The $\log_{10}K'_{ML}$ values of Fe-$HA_{lignite}$ complexes for different size-fractions were compared for performance with several Fe-chelators proposed for agriculture use. The $\log_{10}K'_{ML}$ values of biodegradable Fe-chelators (GLDA, HIDS, EDDS, IDSA, or NTA), which was suggested as the eco-friendly alternatives to classical chelators (EDTA, DTPA, or EDDHA), was lower than those obtained for $HA_{lignite}$ (30–100 kDa) fraction. Hence, despite the fact that the $\log_{10}K'_{ML}$ values for $HA_{lignite}$ size-fractions were lower than the non-biodegradable classical chelators, the organomineral fertilizer enriched with $HA_{lignite}$ (30–100 kDa) fraction could be an economical, eco-friendly alternative to the other synthetic Fe-chelators promoted for similar advantageous characteristics.

Acknowledgment

The research has partially been supported by the Grants-in-Aid for Scientific Research (17K00622 and 15H05118) from the Japan Society for the Promotion of Science.

References

[1] G. Vert, N. Grotz, F. Dédaldéchamp, F. Gaymard, M.L. Guerinot, J.-F. Briat, C. Curie, Plant Cell 14 (2002) 1223-1233.

[2] G.R. Rout, S. Sahoo, Rev. Agric. Sci. 3 (2015) 1-24.

[3] Y. Zuo, F. Zhang, Plant Soil 339 (2011) 83-95.

[4] M. Shenker, Y. Chen, Soil Sci. Plant Nutr. 51 (2005) 1-17.

[5] V. Römheld, H. Marschner, Plant Physiol. 71 (1983) 949-954.

[6] J. Jeong, E.L. Connolly, Plant Sci 176 (2009) 709-714.

[7] H. Marschner, V. Römheld, M. Kissel, J. Plant Nutr. 9 (1986) 695-713.

[8] J.J. Lucena, in: L. Barton, J. Abadia (Eds.), Iron Nutrition in Plants and Rhizospheric Microorganisms, Springer, Dordrecht, Netherlands, 2006, p. 103-128.

[9] M. Villén, A. García-Arsuaga, J.J. Lucena, J. Agric. Food Chem. 55 (2007) 402-407.

[10] A. Wallace, G.A. Wallace, J. Plant Nutr. 15 (1992) 1487-1508.

[11] T. Egli, J. Biosci. Bioeng. 92 (2001) 89–97.

[12] I.M.M. Rahman, M.M. Hossain, Z.A. Begum, M.A. Rahman, H. Hasegawa, in: I.A. Golubev (Ed.) Handbook of Phytoremediation, Nova Science Publishers, New York, 2011, p. 709–722.

[13] I.S.S. Pinto, I.F.F. Neto, H.M.V.M. Soares, Environ. Sci. Pollut. R. 21 (2014) 11893-11906.

[14] Z.A. Begum, I.M.M. Rahman, H. Hasegawa, J. Mol. Liq. 242 (2017) 1123-1130.

[15] Z.A. Begum, I.M.M. Rahman, H. Sawai, S. Mizutani, T. Maki, H. Hasegawa, Water Air Soil Poll. 224 (2013) 1381.

[16] Z.A. Begum, I.M.M. Rahman, Y. Tate, H. Sawai, T. Maki, H. Hasegawa, Chemosphere 87 (2012) 1161–1170.

[17] Z.A. Begum, I.M.M. Rahman, Y. Tate, Y. Egawa, T. Maki, H. Hasegawa, J. Solution Chem. 41 (2012) 1713-1728.

[18] H. Hasegawa, M.A. Rahman, K. Saitou, M. Kobayashi, C. Okumura, Environ. Exp. Bot. 71 (2011) 345-351.

[19] H. Hasegawa, M.M. Rahman, K. Kadohashi, Y. Takasugi, Y. Tate, T. Maki, M.A. Rahman, Plant Physiol. Bioch. 58 (2012) 205-211.

[20] D. Garcia, J. Cegarra, M. Abad, F. Fornes, Bioresource Technol. 43 (1993) 221–225.

[21] K. Chassapis, M. Roulia, D. Tsirigoti, Int. J. Coal Geol. 78 (2009) 288–295.

[22] J. Peuravuori, P. Žbánková, K. Pihlaja, Fuel Process. Technol. 87 (2006) 829-839.

[23] A. Tehranifar, A. Ameri, J. Biol. Environ. Sci. 6 (2012) 77–79.

[24] F. Adani, P. Genevini, P. Zaccheo, G. Zocchi, J. Plant Nutr. 21 (1998) 561–575.

[25] Y. Chen, in: A. Piccolo (Ed.) Humic Substances in Terrestrial Ecosystems, Elsevier Science B.V., Amsterdam, 1996, p. 507-529.

[26] A. Piccolo, G. Pietramellara, J.S.C. Mbagwu, Geoderma 75 (1997) 267–277.

[27] A.K. Pandey, S.D. Pandey, V. Misra, Ecotoxicol. Environ. Saf. 47 (2000) 195–200.

[28] K. Kuma, J. Tanaka, K. Matsunaga, Mar. Biol. 134 (1999) 761–769.

[29] M. Chen, W.X. Wang, Aquat. Biol. 3 (2008) 155–166.

[30] M. Abad, F. Fornes, D. García, J. Cegarra, A. Roig, in: B. Allard, H. Borén, A. Grimvall (Eds.), Humic Substances in the Aquatic and Terrestrial Environment, Springer, Berlin, 1991, p. 391-396.

[31] J.D. Ritchie, E.M. Perdue, Geochim. Cosmochim. Ac. 67 (2003) 85-96.

[32] A. Matynia, T. Lenoir, B. Causse, L. Spadini, T. Jacquet, A. Manceau, Geochim. Cosmochim. Ac. 74 (2010) 1836-1851.

[33] J.F.L. Duval, K.J. Wilkinson, H.P. van Leeuwen, J. Buffle, Environ. Sci. Technol. 39 (2005) 6435-6445.

[34] P. Conte, R. Spaccini, D. Smejkalova, A. Nebbioso, A. Piccolo, Chemosphere 69 (2007) 1032–1039.

[35] H. Hasegawa, Y. Tate, M. Ogino, T. Maki, Z.A. Begum, T. Ichijo, I.M.M. Rahman, J. Appl. Phycol. 29 (2017) 903-915.

[36] G.R. Aiken, in: G.R. Aiken, D.M. McKnight, R.L. Wershaw, P. MacCarthy (Eds.), Humic Substances in Soil, Sediment and Water: Geochemistry and Isolation, Wiley-Interscience, New York, 1985.

[37] K. Tsutsuki, S. Kuwatsuka, Soil Sci. Plant Nutr. 24 (1978) 547-560.

[38] M.T. Beck, I. Nagypal, Chemistry of Complex Equilibria. Ellis Horwood, Chichester, 1990.

[39] M. Jabbari, S. Khosravinia, J. Mol. Liq. 216 (2016) 216-223.

[40] B. Kř'ibek, J. Podlaha, Org. Geochem. 2 (1980) 93-97.

[41] P. Gans, B. O'Sullivan, Talanta 51 (2000) 33–37.

[42] P. Gans, A. Sabatini, A. Vacca, Talanta 43 (1996) 1739–1753.

[43] L. Alderighi, P. Gans, A. Ienco, D. Peters, A. Sabatini, A. Vacca, Coordin. Chem. Rev. 184 (1999) 311–318.

[44] C.F. Baes, R.E. Messmer, The Hydrolysis of Cations. Wiley Interscience, New York, 1976.

[45] A.P. Deshmukh, C. Pacheco, M.B. Hay, S.C.B. Myneni, Geochim. Cosmochim. Ac. 71 (2007) 3533-3544.

[46] M.B. Hay, S.C.B. Myneni, Geochim. Cosmochim. Ac. 71 (2007) 3518-3532.

[47] A.E. Martell, R.M. Smith, R.J. Motekaitis, Texas A&M University, College Station, TX, 2004.

[48] A.E. Angkawijaya, A.E. Fazary, E. Hernowo, M. Taha, Y.-H. Ju, J. Chem. Eng. Data 56 (2011) 532-540.

[49] M. Schnitzer, S.I.M. Skinner, Soil Sci. 99 (1965) 278-284.

[50] V. Cheam, Can. J. Soil Sci. 53 (1973) 377-382.

[51] D.D. Perrin, Nature 182 (1958) 741-742.

[52] E. Giannakopoulos, P. Stathi, K. Dimos, D. Gournis, Y. Sanakis, Y. Deligiannakis, Langmuir 22 (2006) 6863-6873.

[53] A.E. Fazary, M. Taha, Y.-H. Ju, J. Chem. Eng. Data 54 (2009) 35-42.

[54] A.E. Fazary, Y.-H. Ju, J. Solution Chem. 37 (2008) 1305-1319.

[55] H. Powell, M. Taylor, Aust. J. Chem. 35 (1982) 739-756.

[56] P.A. Yeats, P.M. Strain, B.G. Whitehouse, Limnol. Oceanogr. 35 (1990) 1368–1375.

[57] M. Brigante, G. Zanini, M. Avena, Colloid Surface A 347 (2009) 180–186.

[58] R. vonWandruszka, C. Ragle, R. Engebretson, Talanta 44 (1997) 805–809.

[59] A.E. Martell, R.D. Hancock, Metal Complexes in Aqueous Solutions. Plenum Press, New York, 1996.

[60] J. Davidge, C.P. Thomas, D.R. Williams, Chem. Speciation Bioavailability 13 (2001) 129–134.

[61] Z.A. Begum, I.M.M. Rahman, H. Sawai, Y. Tate, T. Maki, H. Hasegawa, J. Chem. Eng. Data 57 (2012) 2723–2732.

[62] H. Hyvönen, M. Orama, H. Saarinen, R. Aksela, Green Chem. 5 (2003) 410-414.

[63] B. Nörtemann, in: B. Nowack, J.M. VanBriesen (Eds.), Biogeochemistry of Chelating Agents, American Chemical Society, Washington, DC, 2005, p. 150–170.

[64] H. Hyvönen, P. Lehtinen, R. Aksela, J. Coord. Chem. 61 (2008) 984-996.

Journal of Molecular Liquids 254: 241-247
The original publication is available at: https://doi.org/10.1016/j.molliq.2018.01.104

Table 1: Characteristics of the lignite-derived humic acid ($HA_{lignite}$) size-fractions

	$HA_{lignite}$ (5–10 kDa)[†]	$HA_{lignite}$ (10–30 kDa)[†]	$HA_{lignite}$ (30–100 kDa)[†]	$HA_{lignite}$ (>100 kDa)[†]
AMW (Da)[a]	1200	2000	2700	4300
TOC (mg L^{-1})[b]	2000	880	1900	2600

[†] The values in the parenthesis indicate the size of the filter used for size-fractionation. The filter size is decided according to the ratios of 'molecular length (size)' and 'molecular weight' of proteins. Although the shape and ratio of humic acids used in the current work were different from the filter size, it has been mentioned to describe the fractionation assembly.

[a] AMW stands for 'average molecular weight' as found in reference to sodium polystyrenesulfonate markers.

[b] TOC stands for 'total organic carbon', which indicate the HA concentrations in a solution that separated directly from the ultrafiltration procedure as shown in the Fig. S1.

Table 2: The proton-binding constants ($\log_{10}\beta$pqr) of $HA_{lignite}$ size-fractions (T, 25 ± 0.1°C; I, 0.1 mol·dm^{-3}; matrix, H_2O)

Formation reactions	p	q	r	$\log_{10}\beta_{pqr}$	SD
$HA_{lignite}$ (5–10 kDa)					
H + HA ⇌ HHA	0	1	1	10.52	0.03
HHA + H ⇌ H_2HA	0	2	1	13.32	0.06
$HA_{lignite}$ (10–30 kDa)					
H + HA ⇌ HHA	0	1	1	10.62	0.06
HHA + H ⇌ H_2HA	0	2	1	13.40	0.09
$HA_{lignite}$ (30–100 kDa)					
H + HA ⇌ HHA	0	1	1	10.37	0.07
HHA + H ⇌ H_2HA	0	2	1	13.41	0.09
$HA_{lignite}$ (>100 kDa)					
H + HA ⇌ HHA	0	1	1	10.66	0.07
HHA + H ⇌ H_2HA	0	2	1	13.33	0.09

[a] The $\log_{10}\beta$pqr values were derived using experimental potentiometric data (n = 3) processed with HYPERQUAD 2008. The p, q, r symbols denote, respectively, the stoichiometric coefficients for metal ions, protons, and chelators associated with the possible equilibria in solution.

Table 3. The overall binding constants ($\log_{10}\beta pqr$) of $HA_{lignite}$ size-fractions with Fe^{3+} (*T*, 25 ± 0.1°C; *I*, 0.1 mol·dm^{-3}; matrix, H_2O)

Formation reactions	Log*K*	*p*	*q*	*r*	$\log_{10}\beta_{pqr}$	SD
$HA_{lignite}$ (5–10 kDa)						
Fe + HA ⇌ FeHA	16.65	1	0	1	16.65	0.07
Fe + 2HA ⇌ $FeHA_2$	11.95	1	0	2	28.60	0.04
$HA_{lignite}$ (10–30 kDa)						
Fe + HA ⇌ FeHA	16.75	1	0	1	16.75	0.11
Fe + 2HA ⇌ $FeHA_2$	12.26	1	0	2	29.01	0.07
$HA_{lignite}$ (30–100 kDa)						
Fe + HA ⇌ FeHA	17.34	1	0	1	17.34	0.11
Fe + 2HA ⇌ $FeHA_2$	11.83	1	0	2	29.17	0.06
$HA_{lignite}$ (>100 kDa)						
Fe + HA ⇌ FeHA	16.58	1	0	1	16.58	0.07
Fe + 2HA ⇌ $FeHA_2$	12.48	1	0	2	29.06	0.05

[a] The $\log_{10}\beta pqr$ values were derived using experimental potentiometric data (n = 3) processed with HYPERQUAD 2008. The *p*, *q*, *r* symbols denote, respectively, the stoichiometric coefficients for metal ions, protons, and chelators associated with the possible equilibria in solution.

Table 4. The stepwise protonation and complexation constants of the ML systems (M, Fe^{3+}; L, $HA_{lignite}^{2-}$) compared with the corresponding values of other chelators (*T*, 25 ± 0.1°C; *I*, 0.1 mol·dm^{-3}; matrix, H_2O).

Chelators†		Stepwise complexation constants (logK_{Fe})						
		$\frac{HL}{[H][L]}$	$\frac{H_2L}{[HL][H]}$	$\frac{H_3L}{[H_2L][H]}$	$\frac{H_4L}{[H_3L][H]}$	$\frac{H_5L}{[H_4L][H]}$	$\frac{ML}{[M][L]}$	$\frac{ML_2}{[M][L]^2}$
$HA_{lignite}$ (5–10 kDa)	$(H_2L)^a$	10.52	2.80	–	–	–	16.65	11.95
$HA_{lignite}$ (10–30 kDa)	$(H_2L)^a$	10.62	2.78	–	–	–	16.75	12.26
$HA_{lignite}$ (30–100 kDa)	$(H_2L)^a$	10.37	3.04	–	–	–	17.34	11.83
$HA_{lignite}$ (>100 kDa)	$(H_2L)^a$	10.66	2.67	–	–	–	16.58	12.48
Salicylic acid	$(H_2L)^b$	13.61	2.98	–	–	–	16.35	11.9
Gallic acid	(H_2L)	8.38[c]	4.10[c]	–	–	–	14.73[d]	11.93[d]
GLDA	$(H_4L)^e$	9.39	5.01	3.49	2.56	–	15.27	–
HIDS	$(H_4L)^e$	9.61	4.07	3.08	2.14	1.6	14.96	–
EDDS	$(H_4L)^f$	10.01	6.84	3.86	2.95	–	22.00[h]	–
IDSA	$(H_4L)^g$	10.52	4.55	3.53	2.43	1.52	13.86	–
NTA	$(H_3L)^f$	9.46–9.84	2.52	1.81	–	–	16.0	24.0
EDTA	$(H_4L)^f$	9.52–10.37	6.13	2.69	2	(1.5)	25.1	–
DTPA	$(H_5L)^f$	9.90–10.79	8.40–8.60	4.28	2.7	2.0	27.7	–
EDDHA	$(H_4L)^f$	12.05	10.87	8.79	6.33	–	35.54	–

[a] Current work, [b] Perrin [51], [c] Fazary, *et al.* [54], [d] Powell, *et al.* [55], [e] Begum, *et al.* [61], [f] Martell, *et al.* [47], [g] Hyvönen, *et al.* [62], [h] *T*, 20 °C

†GLDA: DL-2-(2-carboxymethyl)nitrilotriacetic acid, HIDS: 3-Hydroxy-2,2´-iminodisuccinic acid, EDDS: [S,S]-Ethylenediaminedisuccinic acid, IDSA: Iminodisuccinic acid, NTA: Nitrilotriacetic acid, EDTA: Ethylenediaminetetraacetic acid, DTPA: Diethylenetriaminepentaacetic acid, and EDDHA: Ethylenediamine-*N*,*N*´-bis(2-hydroxyphenylacetic acid)

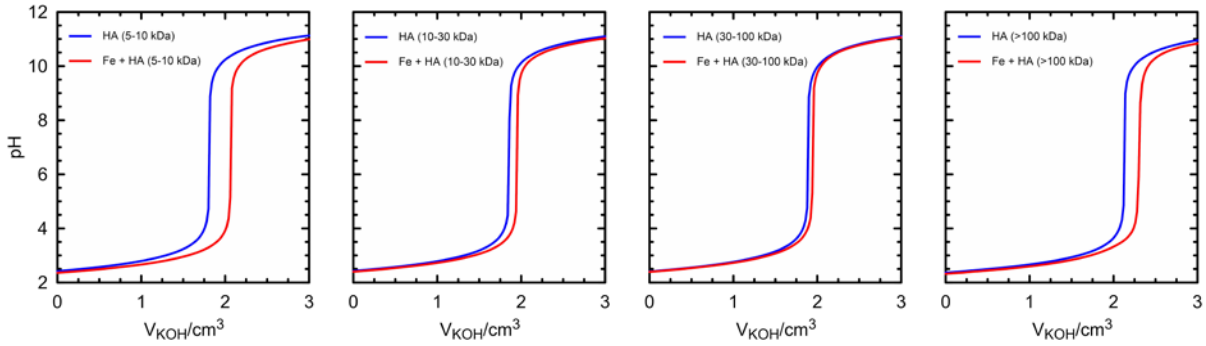

Figure 1: The potentiometric titration curves for the ML systems (M, Fe^{3+}; L, $HA_{lignite}^{2-}$) as a function of titre volume (T, 25 ± 0.1°C; I, 0.1 mol·dm^{-3}; matrix, H_2O)

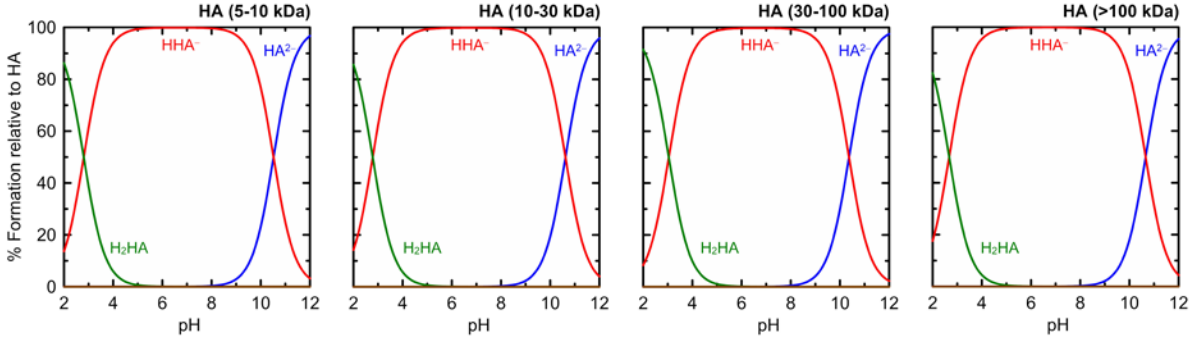

Figure 2: The percentage distribution of different protonation stages of the $HA_{lignite}$ size-fractions (*T*, 25 ± 0.1°C; *I*, 0.1 mol·dm^{-3}; matrix, H_2O)

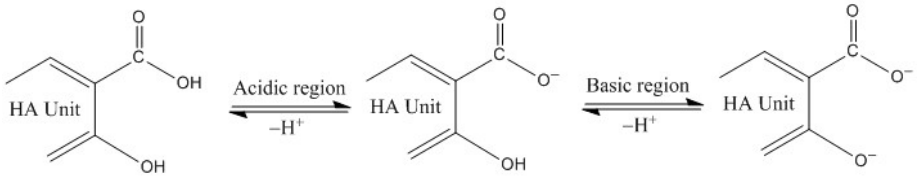

Figure 3: The predicted scheme for the proton-dissociation equilibria of $HA_{lignite}$ size-fractions in different pH-regions (*T*, 25 ± 0.1°C; *I*, 0.1 mol·dm^{-3}; matrix, H_2O)

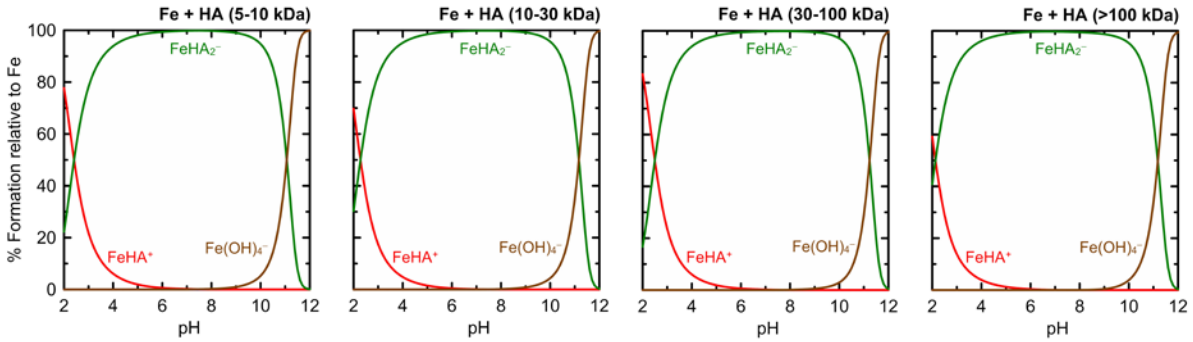

Figure 4: The species distribution curves for Fe^{3+} complexes with $HA_{lignite}$ size-fractions (*T*, 25 ± 0.1°C; *I*, 0.1 mol·dm^{-3}; matrix, H_2O)

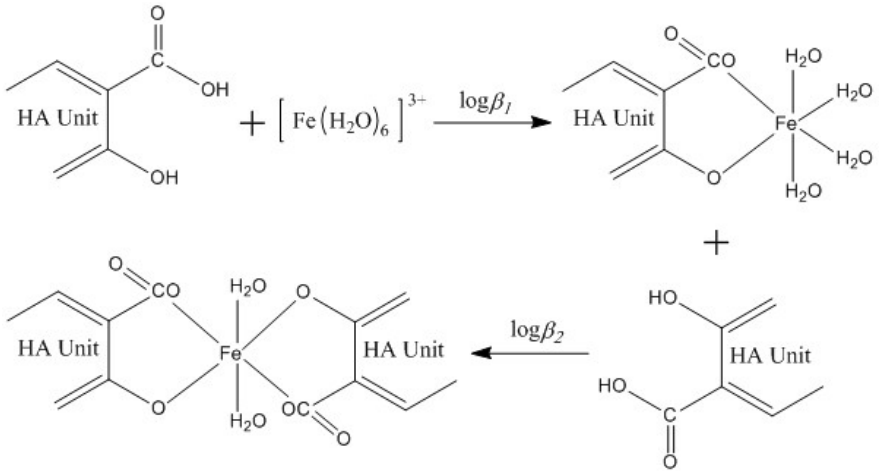

Figure 5: The predicted scheme for the interaction of $HA_{lignite}$ size-fractions with Fe^{3+} ions based on the concept of single reactive structural units (RSU) in different pH-regions

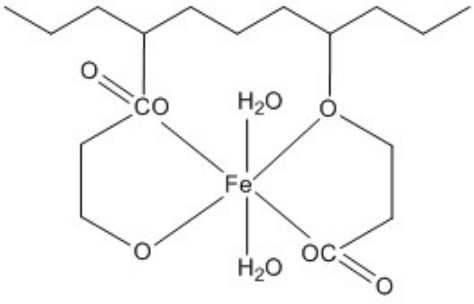

Figure 6: The predicted structure for the interaction of multiple $HA_{lignite}$ size-fractions with a single Fe^{3+} ion based on the concept of reactive structural units (RSU)

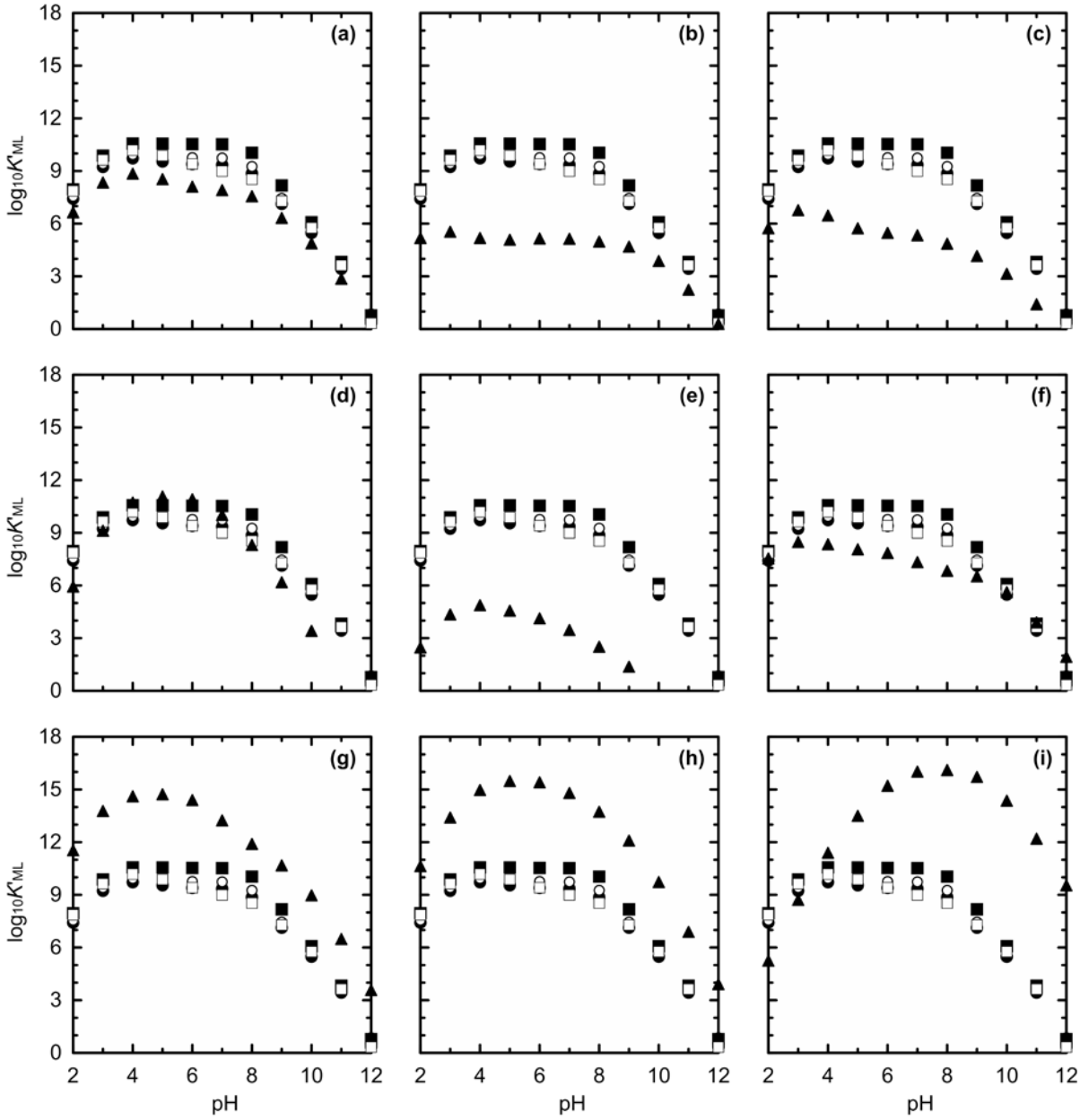

Figure 7: The conditional stability constants ($\log K'_{ML}$) for the Fe-complexes with $HA_{lignite}$ size-fractions [(a)–(i); ●, $HA_{lignite}$ (5–10 kDa), ○, $HA_{lignite}$ (10–30 kDa), ■, $HA_{lignite}$ (30–100 kDa), □, $HA_{lignite}$ (>100 kDa)] and iron-chelators [▲, (a) Salicylic acid, (b) GLDA, (c) HIDS, (d) EDDS, (e) IDSA, (f) NTA, (g) EDTA, (h) DTPA, (i) EDDHA] as a function of pH (T, 25 ± 0.1°C; I, 0.1 mol·dm^{-3}; matrix, H_2O).